DECEMBER 1983 LRP 230/83

IDEAL MHD BETA LIMITS FOR INTOR

F. Troyon, R. Gruber, and H. Saurenmann,

Contract 087/81-12/FU-CH/NET. Final Report

IDEAL MHD BETA LIMITS FOR INTOR

F. Troyon, R. Gruber, and H. Saurenmann

ABSTRACT

Ideal MHD stability considerations limit the range of operation of Tokamaks. Without invoking an eventual stabilisation by a shell the onset of n = 1 instabilities and ballooning modes limit the maximum β which can be confined with a given current. This limit is determined for a class of INTOR-like plasmas, keeping the geometry fixed and varying the toroidal current I. A limited profile optimisation is carried out for each value of the current in order to maximize the volume averaged β. It is found that the limiting β increases essentially linearly with the current in the range $q_S>2$ ($q_I>1.6$), reaching 3.7 %.

Contract 087/81-12/FU-CH/NET, Final Report.

1. INTRODUCTION

In the set of parameters which is now accepted as the standard set for symmetric INTOR (Table 1), there are two, the current and β, which are critical. For technical reasons the current should be kept as low as possible, while reaching the ignition requires a minimum value of the averaged β which has been estimated to be of the order of 5.5 %. This implies a very high value of $\beta_I \approx 2.5$. Although the current of 6.4 MA is already high and an increase might be difficult to be accepted because of the added risk in case of major disruptions, it is worthwile to investigate if such an increase could, by a decrease of the required β_I, ease the stability requirement and, in a more general context, to determine the relation between the maximum β and the current. This is the subject of this report which summarizes the work done in the last year and which completes the preliminary study already reported [1]. In order to facilitate comparisons with previous results and because of the time required to do parametric scans we have chosen to keep the same parameters as in our previous studies, which differ slightly from those of Table 1 by having a radius a = 1.3 m instead of 1.2 m and a triangularity γ of 0.3 instead of 0.2.

The plasma shape is given by the parametric equations

$$r = R + a\cos(\theta + \gamma\sin\theta)$$
$$Z = E\,a\sin\theta \qquad (1)$$

The pressure p and the toroidal field B_Φ are represented in terms of the flux function Ψ as

$$p \equiv p_0\tilde{\Psi}^2 + p_1\tilde{\Psi}^3$$
$$rB_\phi \equiv \sqrt{t\tilde{\Psi}^2 + R^2B_T^2} \qquad (2)$$

where $\tilde{\Psi} = \Psi - \Psi_S$, Ψ_S is the total flux in the plasma.

Compared to the last INTOR set of parameters the differences are on the plasma radius and on the shape which is here symmetric with a rather high triangularity. The trend of the results is not affected by these changes although the value of β may change somewhat. A more important factor could be the presence of a divertor and of the separatrix since it appears that it is the safety factor at the edge, q_S, which limits the current.

The free parameters p_0, p_1 and t control the total current I, the safety factor on axis q_0 and the volume averaged $\beta \equiv \int pdV/\int B^2/2dV$ or, equivalently, $\beta_J \equiv 8\pi\int pdS/I^2$ (INTOR convention).

The results of the study can be summarized in the following way :

- For a given current the optimum profiles, which give the highest β stable to n = 1 free boundary perturbations and satisfying the Mercier and the ballooning criteria, are characterized by $q_0 \sim$ 1.0 - 1.2.

- In this range of q_0 the ballooning limit is close to either the Mercier limit or the n = 1 free boundary limit.

- The results in the range, 4.7 MA $\leq$ I $\leq$ 9.4 MA, are compatible with a β limit given by

$$\beta_{max}(\%) \approx 0.38\ I(MA)$$

which imply a β_J limit given by

$$\beta_{J\ max} \approx 7.5/I(MA).$$

- The behaviour at higher current is not known except that no stable region has been found yet for 10.6 MA.

- The optimum for I $\approx$ 7.2 MA, corresponding to q_s (s = surface) close to 3.0 is very sensitive to q_0, contrary to the other cases.

- If only the ballooning limit is concerned, much higher β values are obtainable but the profiles are completely different, characterized by large values of q_0 (lower current density on axis, tendency to hollow profiles).

2. DESCRIPTION OF THE PROCEDURE

The equilibria are computed on a rectangular r, z mesh by solving the grad-Schlüter-Shafranov equation adjusting p_0 while keeping p_1/p_0 and t/p_0 constant in order to have the current at a predetermined

sity and the toroidal field at the magnetic axis, is less than 10^{-4}, convergence will lead to the marginal state within the attainable numerical accuracy which is of the order of 10^{-5}. Since such a small residual growthrate is probably beyond the validity of the model and of the accuracy of the equilibrium we have chosen to take 10^{-4} with a 60/60 resolution as the stability limit. This is a procedure suggested for the same physical reasons by Goedbloed and Sakanaka [3] and known as σ-stability.

The ballooning criterion used in ERATO is based on a variational formulation of the ballooning equation. The angular domain studied has been limited to a range of 100 short turns as the numerical inaccuracies of the equilibrium lead to incredible results when one tries to exceed appreciably this number. Near the magnetic axis this is usually not sufficient. For example, in many cases where the Mercier criterion is weakly violated on a given magnetic surface close to the axis, which implies that the ballooning criterion is also violated on this surface, we do not find ballooning instability with 100 turns. But, since we know that, asymptotically, increasing the number of turns only gives a negative contribution to the plasma potential energy if the Mercier criterion is violated on that surface, we can use the Mercier criterion itself as an equivalent formulation of the ballooning criterion. Practically, it means that, whenever we do not find a ballooning instability on a given surface with 100 turns, we check the Mercier criterion on this same surface and only consider the plasma as stable if it is satisfied. In most cases, the Mercier criterion is most stringent on the magnetic axis.

value. We then test the stability of each equilibrium with ERATO [2] which provides us with the growthrate of the fastest n = 1 mode in the absence of a shell, a test of the Mercier criterion and the stability index against the ballooning modes on a large number (usually 60) of flux surfaces.

The difficulty to determine numerically the stability limit has been discussed in some detail in ref. [1]. It is of a fundamental nature and it is not related to any specific spectral code. Each time there is a singular surface in the plasma the spectrum of eigenvalues extends to the marginal value $\omega^2 = 0$. If there are more than one singular surfaces the degeneracy of the continuum increases. The discretisation inherent to any numerical scheme replaces the continuum by a dense discrete spectrum but the lowest value is not in general at the marginal point $\omega^2 = 0$. It is well known that ERATO leads, for Tokamak profiles caracterized with $q' > 0$, to an error due to the numerical discretisation which is negative and thus destabilizes the lower edge of the continuum. For a given resolution the plasma appears to be unstable. It is then necessary to do a convergence study as a function of mesh size in order to verify if the equilibrium is unstable or marginal. It has been found that the convergence is monotonic at sufficiently high resolution although it can have strong breaks,whenever resolution brings out the sharper features of the eigenmodes which inevitably arise at very low growthrates since the mode looks more and more like a singular mode of the continuum edge. Experience has shown that if, with a resolution of 60 radial surfaces and 60 azimuthal points, the square of the fastest growthrate Γ^2, normalized to the Alfvén transit time across the major radius calculated with the den-

3. RESULTS

3.1 Standard case, I = 5.9 MA

The stability diagram for the "standard" case already given in [1] is shown in Fig. 1 in the (β, q_0)-plane. The safety factor at the plasma surface, q_s, varies little around 3.5 over the whole parameter range. The curves labeled by a number correspond to a constant growthrate of the n = 1 free boundary mode obtained with the same 60/60 mesh. The label is the square of the growthrate Γ^2, normalized to the Alfvén transit frequency $\omega^2_A \equiv B^2_T/(R^2_0 \rho_0)$, ρ_0 being the density, chosen constant, and R_0 the radius of the magnetic axis. Stability, according to our convention, is below the curve labeled 10^{-4}. Note that this n = 1 free-boundary instability really provides a β-limit. The rapid increase of the growthrate as the stability boundary is crossed is a measure of the "hardness" of the limit. The global character of the instability is apparent on the map of the poloidal flow in two meridian planes separated by 90^0 shown in Fig. 2, the values of the parameters of this case being shown in Fig. 1 as point A1. The ballooning nature of the mode is visible, the number of vortices increasing in parallel with q as one moves from the axis to the surface. Near the axis the mode is m = 1, becoming mainly m = 2 near q = 2 and m = 3 at the surface.

When q_0 drops substantially below 1 there is also a n = 1 instability, which is essentially an internal kink, with a growthrate which increases as q_0 decreases. The mode also becomes less localized as q_0 decreases, with larger activity at the other singular surfaces and at

for the modes localized near the magnetic axis where our ballooning criterion is no longer accurate. As the Mercier limit M is crossed the Mercier unstable domain grows from the magnetic axis.

In an equilibrium optimized for ballooning stability the B and M limits would coincide since the ballooning criterion would become violated everywhere simultaneously. But the ballooning limit is a $n = \infty$ rigid boundary limit so that such an optimisation would only make sense if a small number of low-n free-boundary modes have to be wall-stabilized. Using the same definition of σ-stability we have computed the free-boundary stability limits for n = 2 and n = 4. The result is shown in figure 6 on which the n = 1 and the ballooning limits are repeated for comparison. The conclusion seems to be that wall-stabilization for low-n modes is not useful to increase the limiting β. It is doubtful that even n = 1 and n = 2 could be wall stabilized with the complicated wall structure of INTOR. The conclusion from this study is that the n = 1 free boundary mode limits β. The optimum is at the intersection with the ballooning limit, which is not very different from the intersection with the Mercier limit. Above this limiting β the higher n modes become also unstable so that it seems not to be posible to gain by local profile changes.

3.2 Dependence of the stability limits on the current

We have repeated the optimisation for various currents ($4.7\ \text{MA} \leq I \leq 9.4\ \text{MA}$), concentrating on the parameter range near the optimum, which corresponds in all cases to the intersection of the ballooning and n = 1 free boundary limit and is not very far from the Mercier limit. The results are shown in Fig. 7. The calculation for $n \neq 1$ was not

the plasma surface. Nevertheless the $q_0 \approx 1$ stability boundary appears rather "soft". A map of the poloidal flow in two meridian planes for the unstable case labeled as A2 in Fig. 1 is shown in Fig. 3. It is an internal kink with some motion on the q = 2 and q = 3 surfaces and rather small deformation of the plasma surface. Internal kinks have typically Γ^2 of the order of 10^{-4} or less. Therefore taking the σ-stability limit at 10^{-4} may be optimistic. But this is not important since the Mercier limit, labeled in Fig. 1 as M, constraints q_0 to stay above 1. A series of equilibria, labeled C1 to C5 in Fig. 1, which all lie on or very near the n = 1 stability limit, is shown in Fig. 4. The q profile does not seem an important factor, the β decreasing rather slowly as q_0 increases giving flatter q profiles.

The ballooning limit is shown in Fig. 1 as B, while the Mercier limit is labeled M. There is stability to ballooning modes everywhere below B and to the right of M. When β is increased above the ballooning limit the first unstable magnetic surfaces appear somewhere between the axis and the plasma surface. The unstable domain widens progressively. This limit should be considered as a soft limit since a small reduction of the pressure gradient in the critical region compensated by a redistribution to a more exterior region would stabilize these ballooning modes with no reduction in β. We have not pursued this road. A sequence of equilibria near the ballooning limit B, labeled D1 to D3 in Fig. 1, is shown in Fig. 5, which confirm the trend found in most previous studies that lower shear provides higher β stable to ballooning. We are clearly in the first region of stability. The Mercier limit, in view of the discussion in the precedent section, should also be considered as another ballooning limit, but

repeated since it is highly time consuming and, since the n = 1, M and B limits have always the same qualitative behaviour, we do not expect a different result from the standard case. The general behaviour is similar; but for the case 7.1 MA, which corresponds to q_s around 3, stability is only achieved within a narrow range of q_0. It suggests that the crossing of the q_s = 3 limit should be done carefully after $q_0 \approx 1$ has been reached (sawtooth regime). Because of the computational effort involved we could not investigate the immediate vicinity of this value to find out how rapidly the stable q_0 window enlarges as the current changes around this value. No similar phenomenon was seen around q_s = 4. At the highest current, $q_s \approx 2.2$, the optimal profile is represented in Fig. 8. The q profile is very flat over most of the plasma. It was not possible to extend the diagram beyond q_s = 2 but we do not claim it is not possible. The parametric form chosen does not allow it but a more general form might do better. We have noted that at high current (8.3 and 9.4 MA) the highest stable β equilibria have $t \sim 0$, namely $\beta_p \approx 1$. The increase in β associated with the increase of the current is due to a hollowing of the radial current distribution necessary to keep q_0 near 1, which leads to larger pressure gradient in the outer region without triggering the ballooning instabilities.

The maximum value of β stable to all MHD modes for each value of the current is reported in Fig. 9 versus the current. This limiting β, designated as β_{max}, is reasonably well fitted by the linear relation

$$\beta_{max}(\%) \approx 0.38\ I\ (MA),$$

up to I=9.4 MA, corresponding to q_s=2.2, or $q_I \equiv \pi B_T a^2 (1+E^2)/(\mu_0 IR)$=1.6.

This limit translates into a limit on β_J

$$\beta_J \approx 7.5/I(MA).$$

4. DISCUSSION

The optimisation of the pressure and current profiles has been made with a simple polynomial expression. Attempts at improving the β limit by adding higher order terms have been made for the standard case with no appreciable changes in the optimal value. The calculation has not been repeated for other values of the current, but, in calculations made for JET the same fall-off of the curve at high current has been seen and more terms have been introduced with no success in either pushing the limit to higher β at the highest current or in extending the curve to higher current. Drastically different profiles with more freedom to change profiles locally may be a better road towards improving these results.

The values of β found here are in no contradiction with previous results [4,5]. Our class of profiles covers those used in [4] in which the objective was more towards studying the influence of the geometry. In [5], p' and TT' were set proportional to each other, giving different profiles. It was pointed out by Dr. J. Wesson that the results for a JET shape given in [5], when crossplotted against the current I, gave also a linear dependance of β_{max} vs I for moderate currents, with a drop at higher current.

This work has been carried out under the NET/INTOR contract 087/81-12/FU-CH/NET.

REFERENCES

[1] IAEA-CN-41/P-1-2 and INTOR phase II

[2] R. Gruber, F. Troyon, D. Berger, L.C. Bernard, S. Rousset, R. Schreiber, W. Kerner, W. Schneider, K.V. Roberts, Comp. Phys. Commun. 21 (1981) 323.

[3] J.P. Goebloed, P.H. Sakanaka, Phys. Fluids 17 (1974) 908.

[4] A.M. Todd, J. Manickam, M. Okabayshi, M.S. Chance, R.C. Grimm, J.M. Greene, J.L. Johnson, Nucl. Fusion 19 (1979) 743.

[5] W. Kerner, P. Gautier, K. Lackner, W. Schneider, R. Gruber, F. Troyon, Nucl. Fusion 21 (1981) 1383.

TABLE 1

Reference Parameters of symmetric INTOR, Phase IIA

major radius	= R = 5.2 m
small radius	= a = 1.2 m
elongation	= E = 1.6
triangularity	= γ = 0.2
toroidal field at R	= B_T = 5.5 T
current	= I_T = 6.4 MA
averaged β	= β = 5.5%

FIGURE CAPTIONS

Fig. 1 : Stability diagram for the standard case with I = 5.9 MA. M = Mercier limit, B = ballooning limit; the labeled lines are equilibria with constant growthrate of the free-boundary kink n = 1. The line 10^{-4} is the σ-stability limit for n = 1. The label is the square of the normalized growthrate Γ^2.

Fig. 2 : Map of the n = 1 unstable poloidal flow in two perpendicular meridian planes for an equilibria much above the β-limit (designated as A1 in Fig. 1). The major axis is to the left.

Fig. 3 : Map of the n = 1 unstable poloidal flow in two perpendicular meridian planes for the equlibrium A2 with $q_0 < 1$.

Fig. 4 : Profiles of equilibrium quantities (pressure p, safety factor q, current density in mid-plane j) for a set of marginal equilibria, shown in Fig. 1 as C1 to C5. The horizontal axis R is the major radius normalized to 1 on the magnetic axis. The pressure is normalized to the magnetic pressure on axis $B^2/2$. The scale for j is in arbitrary units.

Fig. 5 : Profiles of equilibrium quantities for a set of equilibria, shown in Fig. 1 as D1 to D3, which all lie on the ballooning limit B. The meaning of the symbols is the same as in Fig. 4.

Fig. 6 : The n = 1, n = 2 and n = 4 free-boundary σ-stability limits for the standard case.

Fig. 7 : Stability diagrams for increasing values of the current: I = 4.7, 6.5, 7.1, 8.3 and 9.4 MA. The curve labeled 10^{-4} is the free boundary σ-stability limit.

Fig. 8 : The highest β fully stable equilibrium found in the study, obtained with I = 9.4 MA, q_0 = 1.25, β = 3.75 %. The quantities shown are the same as in Fig. 4.

Fig. 9 : Maximum fully stable value of the volume averaged β as a function of the current I, or of the safety factor at the plasma surface q_s.

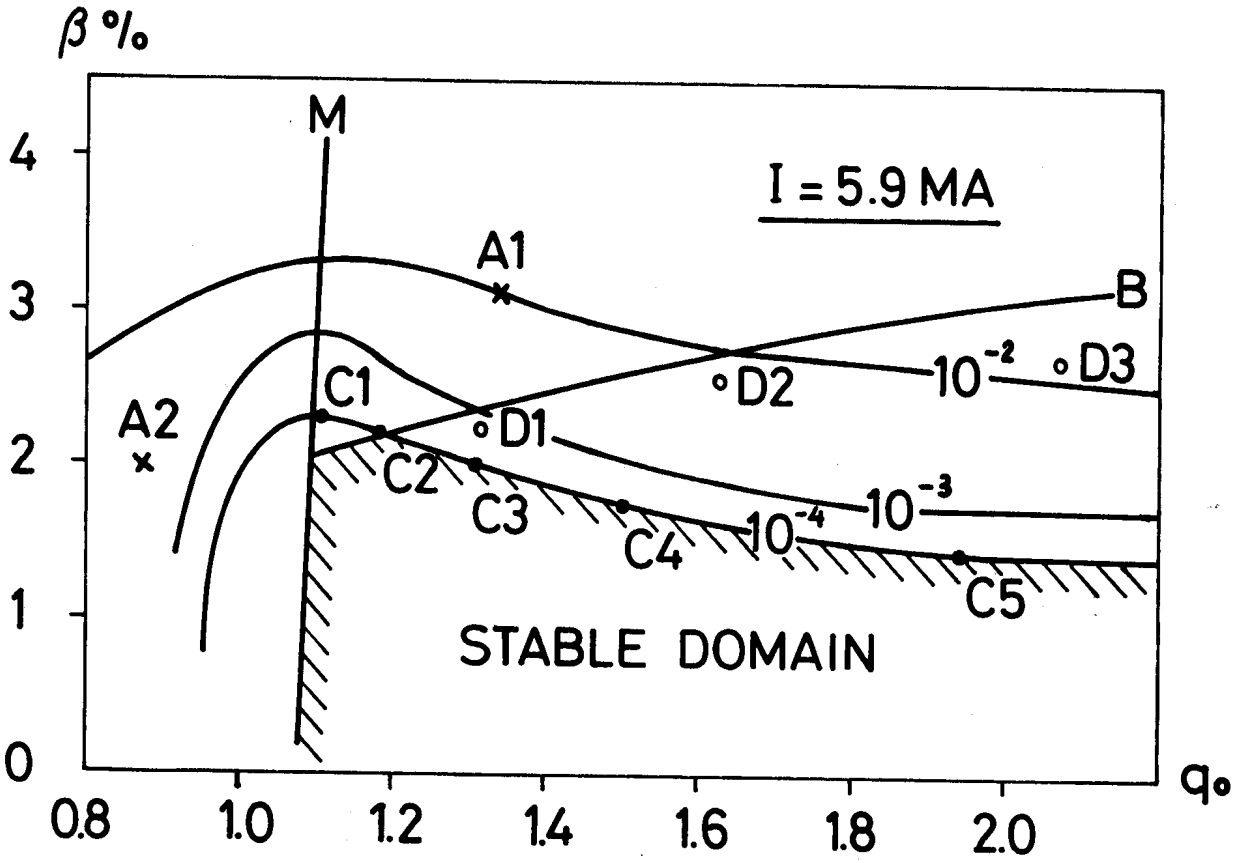
β %
4
3
2
1
0
M
I = 5.9 MA
A1
B
A2
C1
D2
10^-2
D3
D1
C2
C3
10^-3
C4
10^-4
C5
STABLE DOMAIN
0.8
1.0
1.2
1.4
1.6
1.8
2.0
q₀

FIG. 1

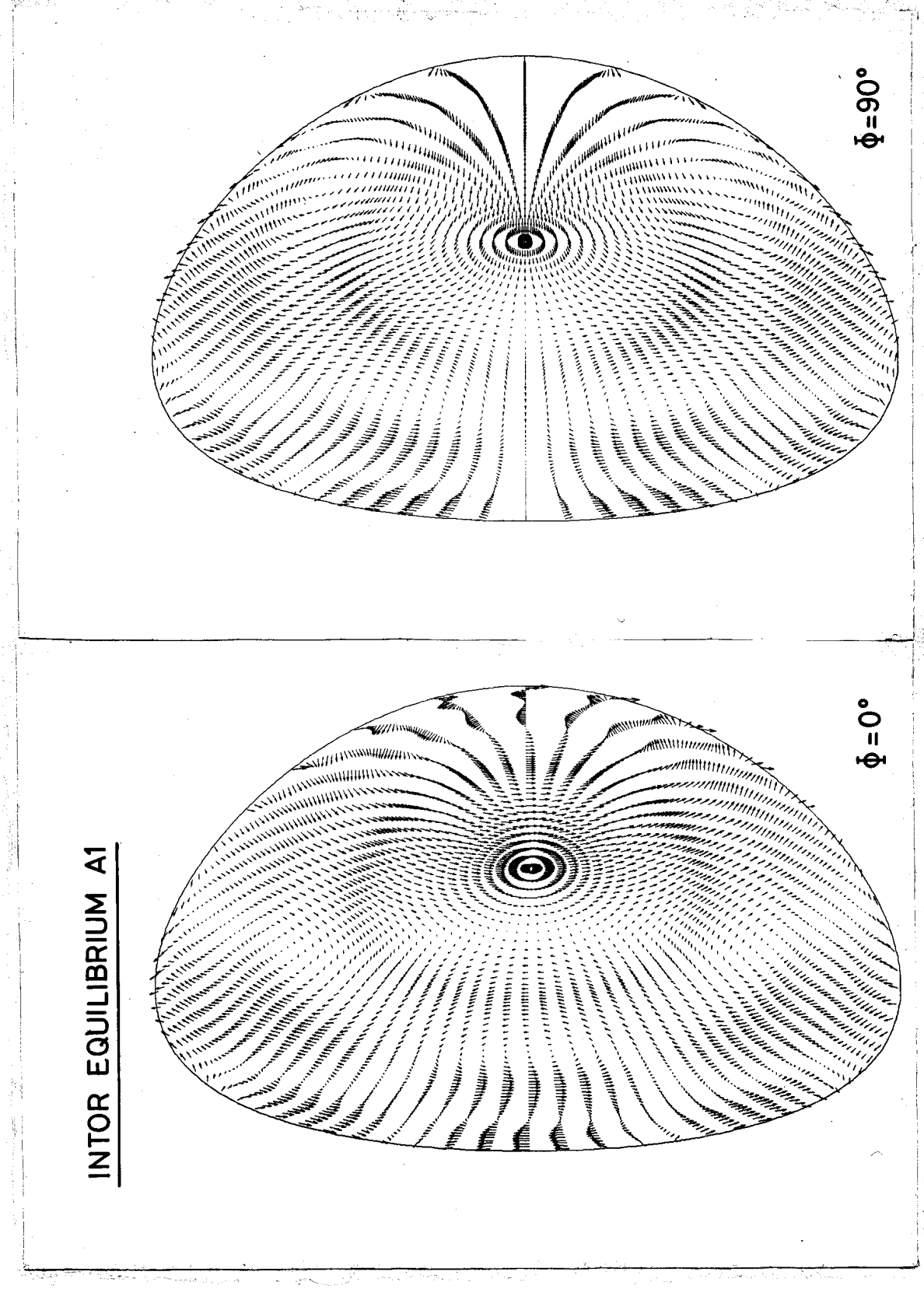

FIG. 2

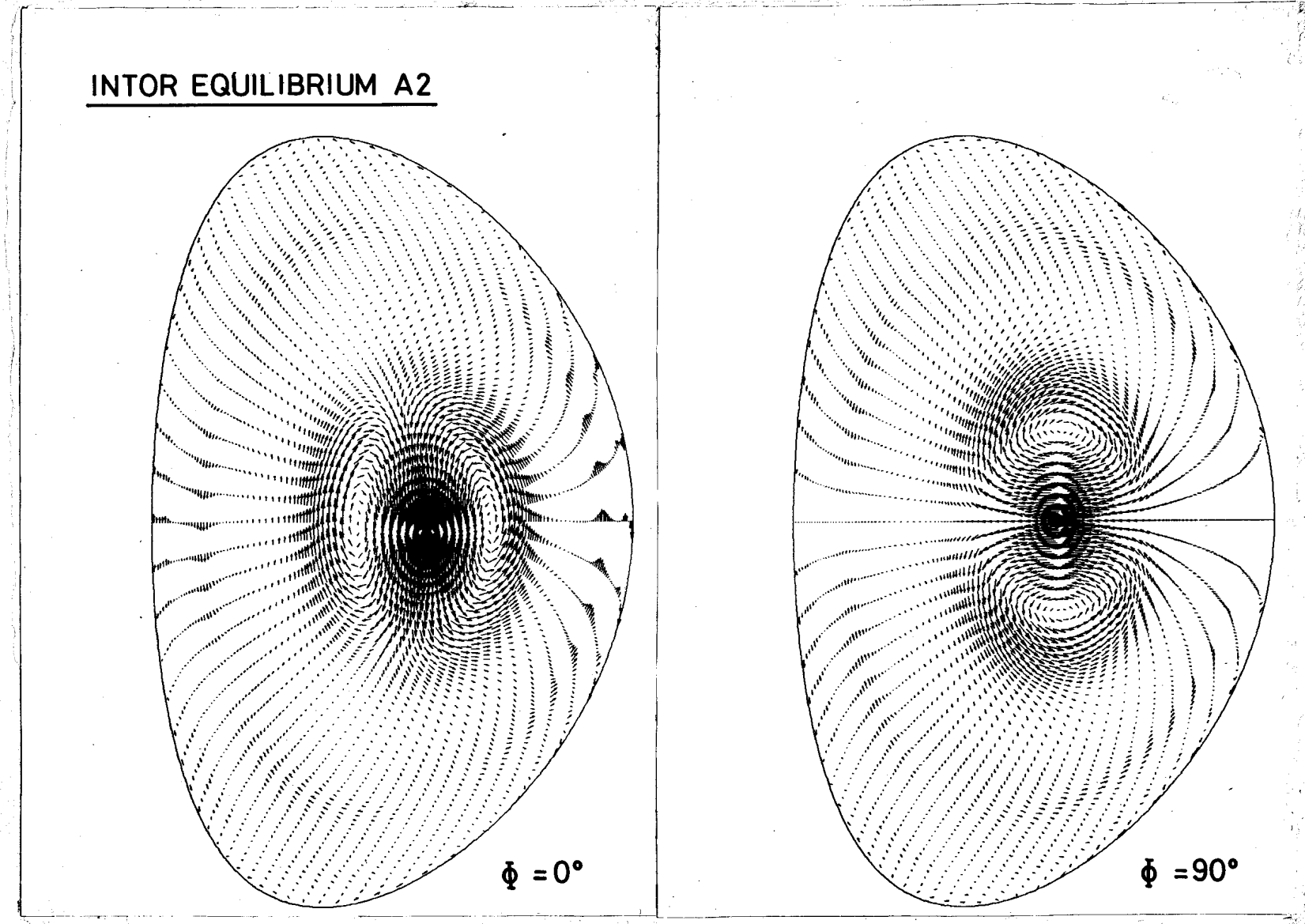

FIG. 3

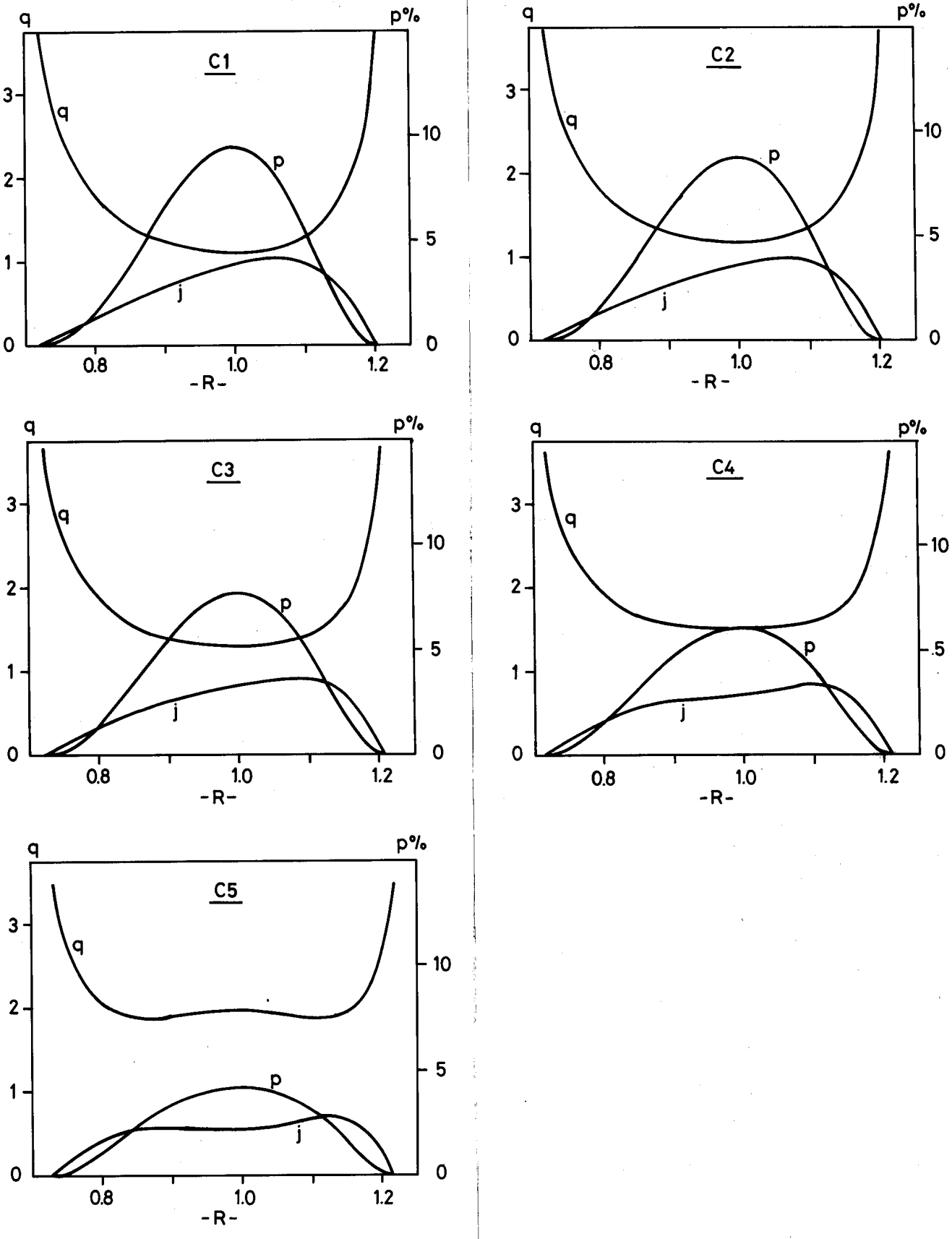

FIG. 4

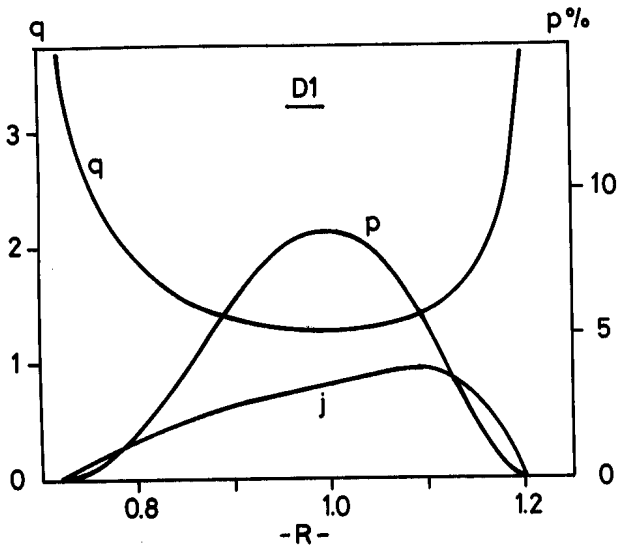
q
p%
D1
q
p
j
3
2
1
0
10
5
0
0.8
1.0
1.2
-R-

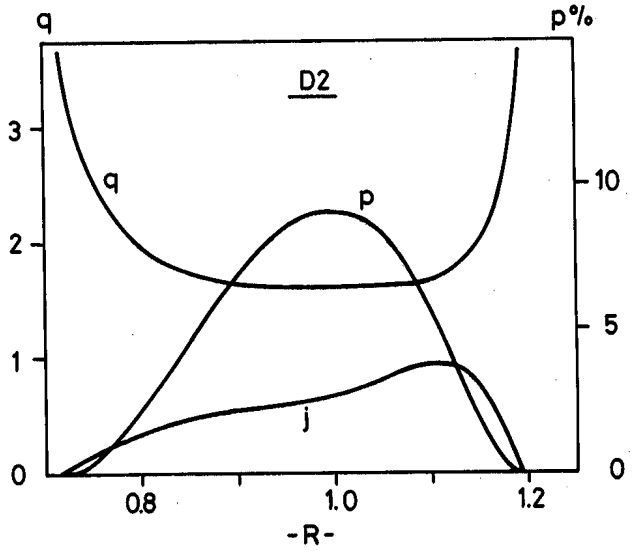
q
p%
D2
q
p
j
3
2
1
0
10
5
0
0.8
1.0
1.2
-R-

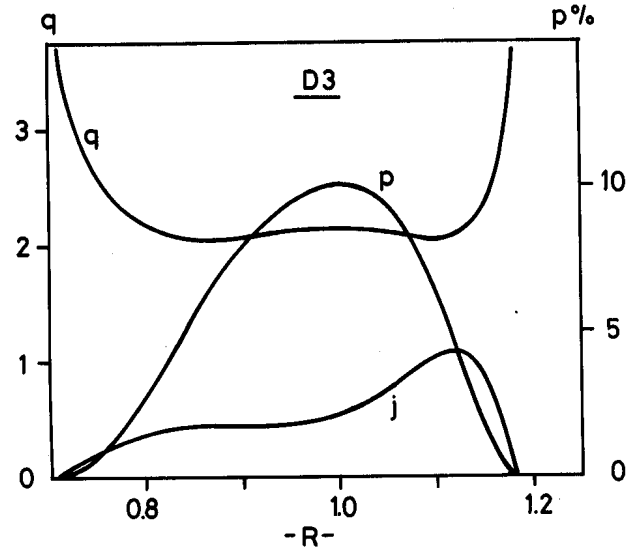
q
p%
D3
q
p
j
3
2
1
0
10
5
0
0.8
1.0
1.2
-R-

FIG. 5

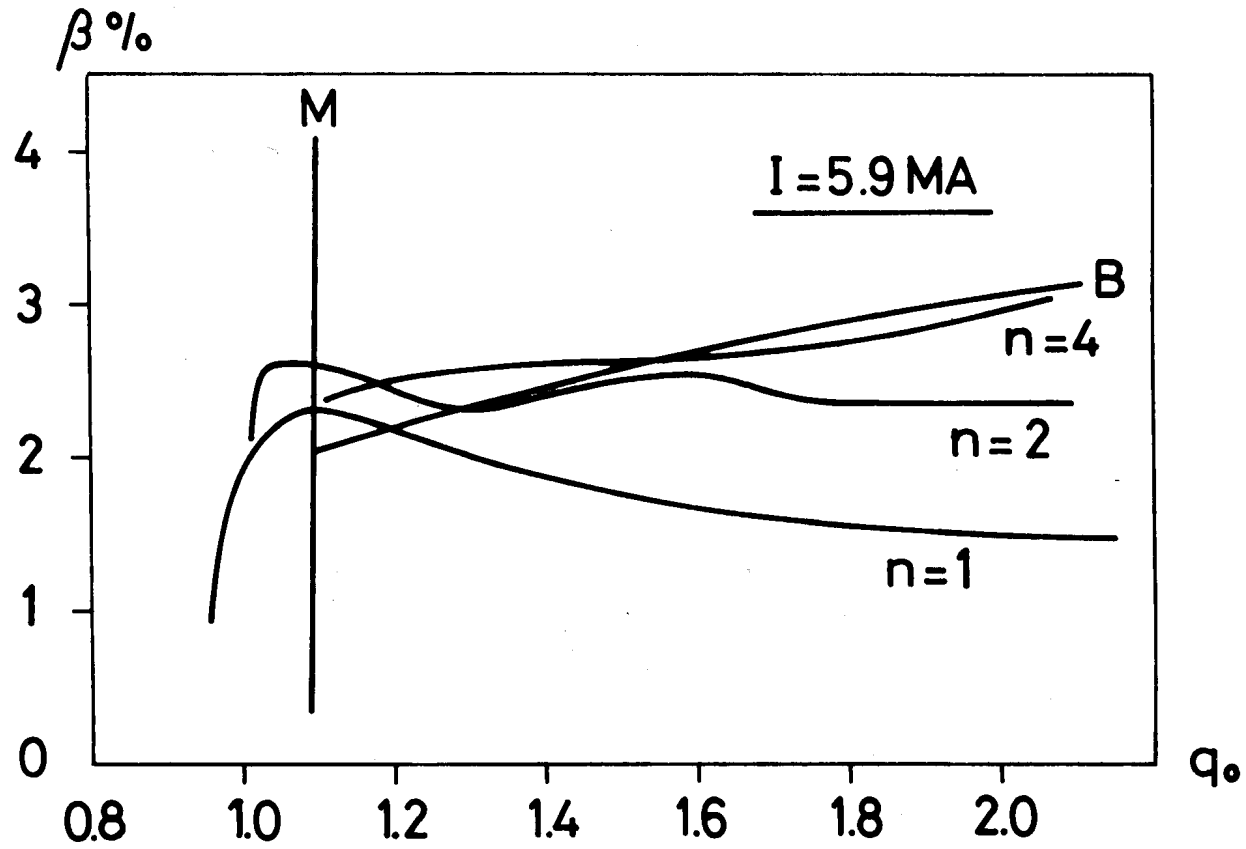

FIG. 6

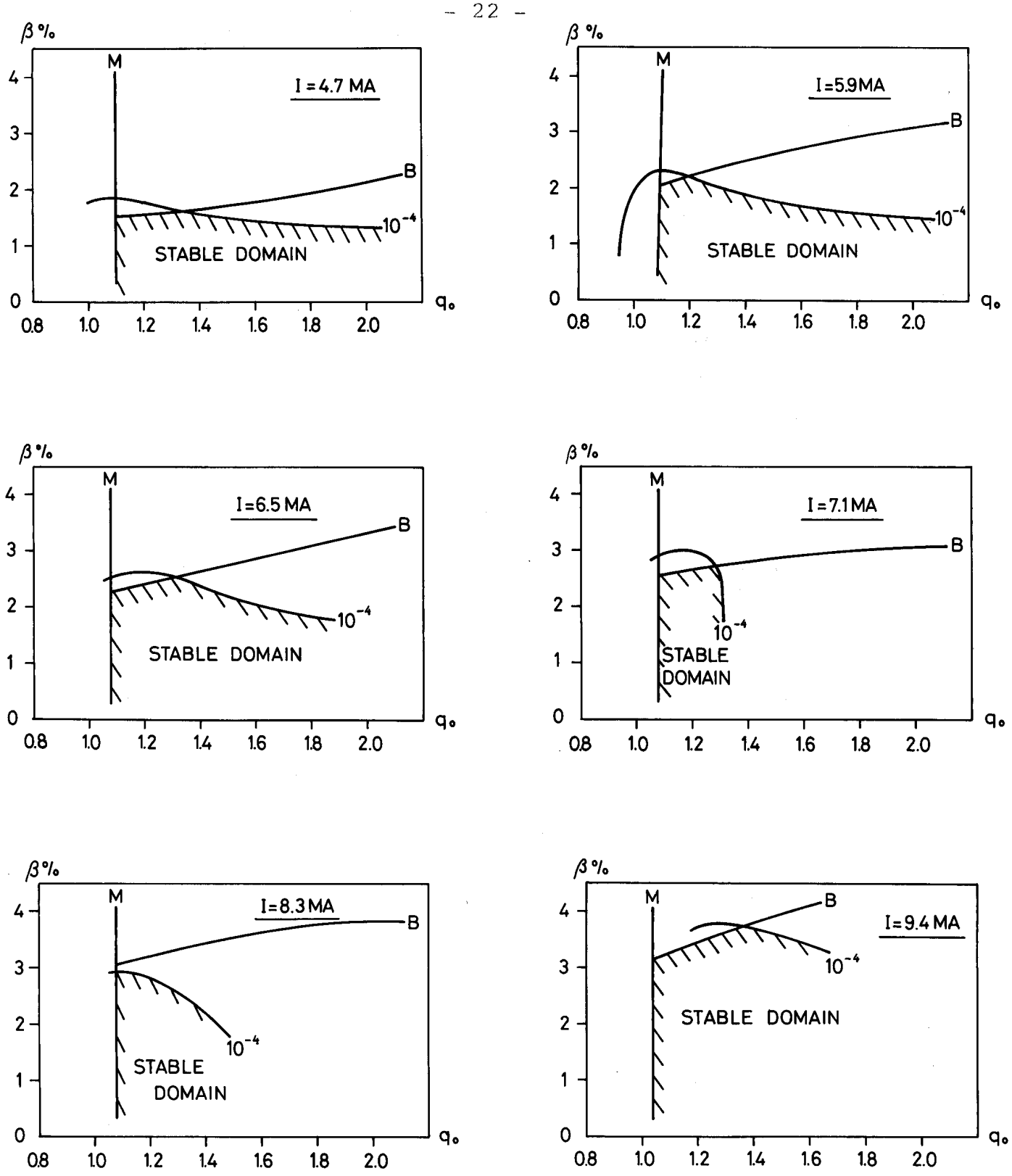
β %
M
I = 4.7 MA
B
10⁻⁴
STABLE DOMAIN
q₀
I=5.9MA
I=6.5 MA
I=7.1MA
STABLE
DOMAIN
I=8.3MA
I=9.4 MA
0.8
1.0
1.2
1.4
1.6
1.8
2.0

FIG. 7

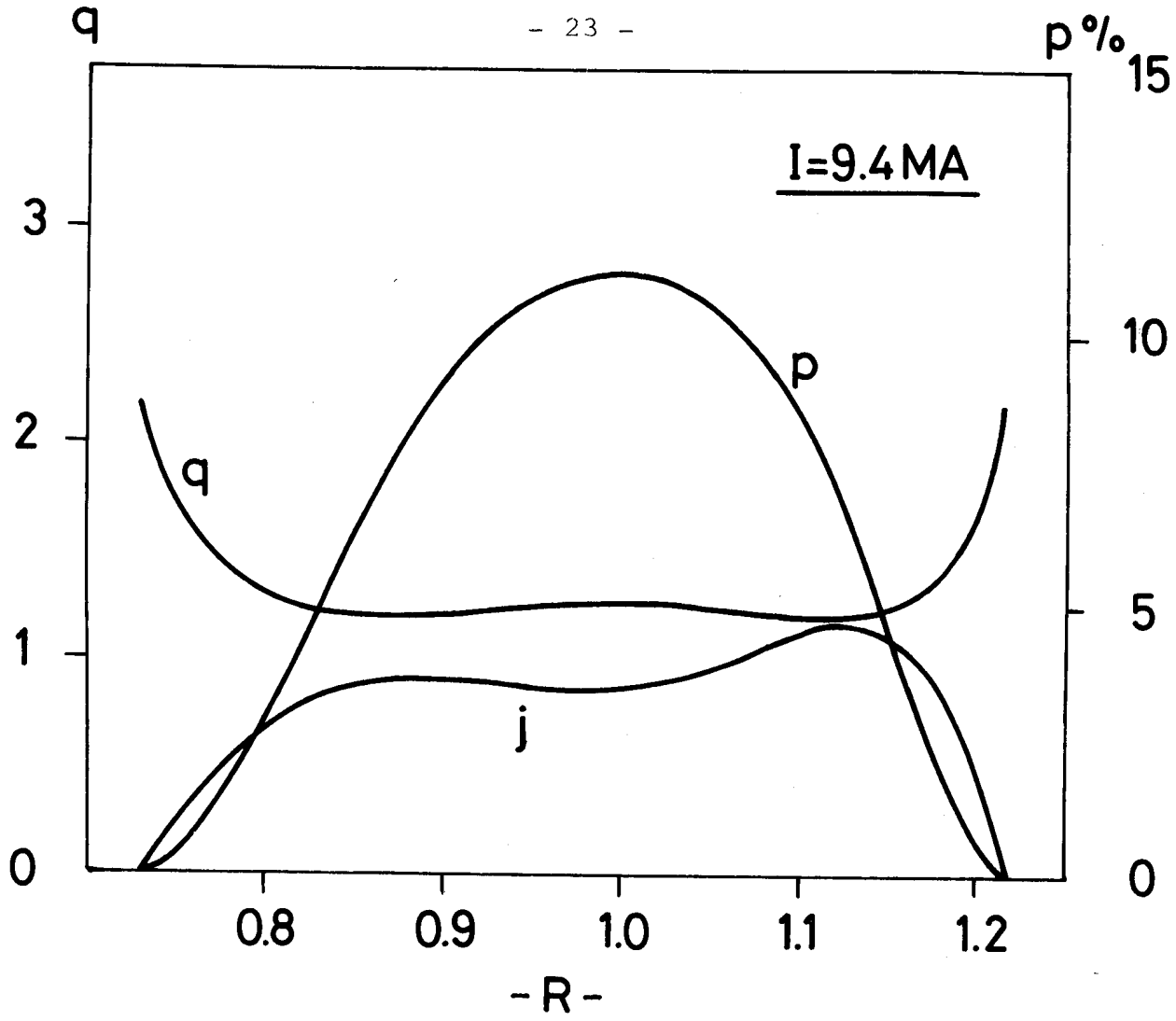
q
p %
15
I=9.4 MA
3
2
1
0
10
5
0
p
q
j
0.8
0.9
1.0
1.1
1.2
- R -

FIG. 8

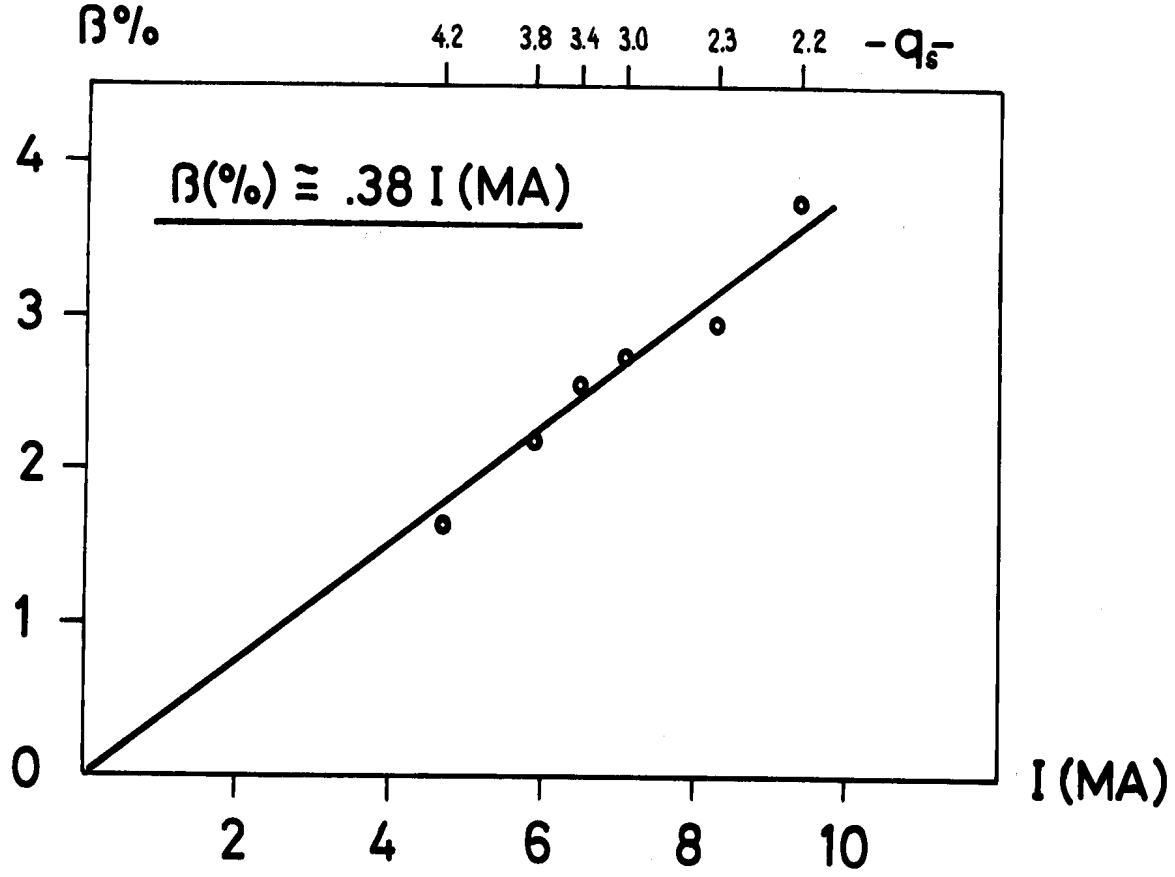
β%
4.2
3.8
3.4
3.0
2.3
2.2
- q_s -
β(%) ≅ .38 I (MA)
4
3
2
1
0
2
4
6
8
10
I (MA)

FIG. 9

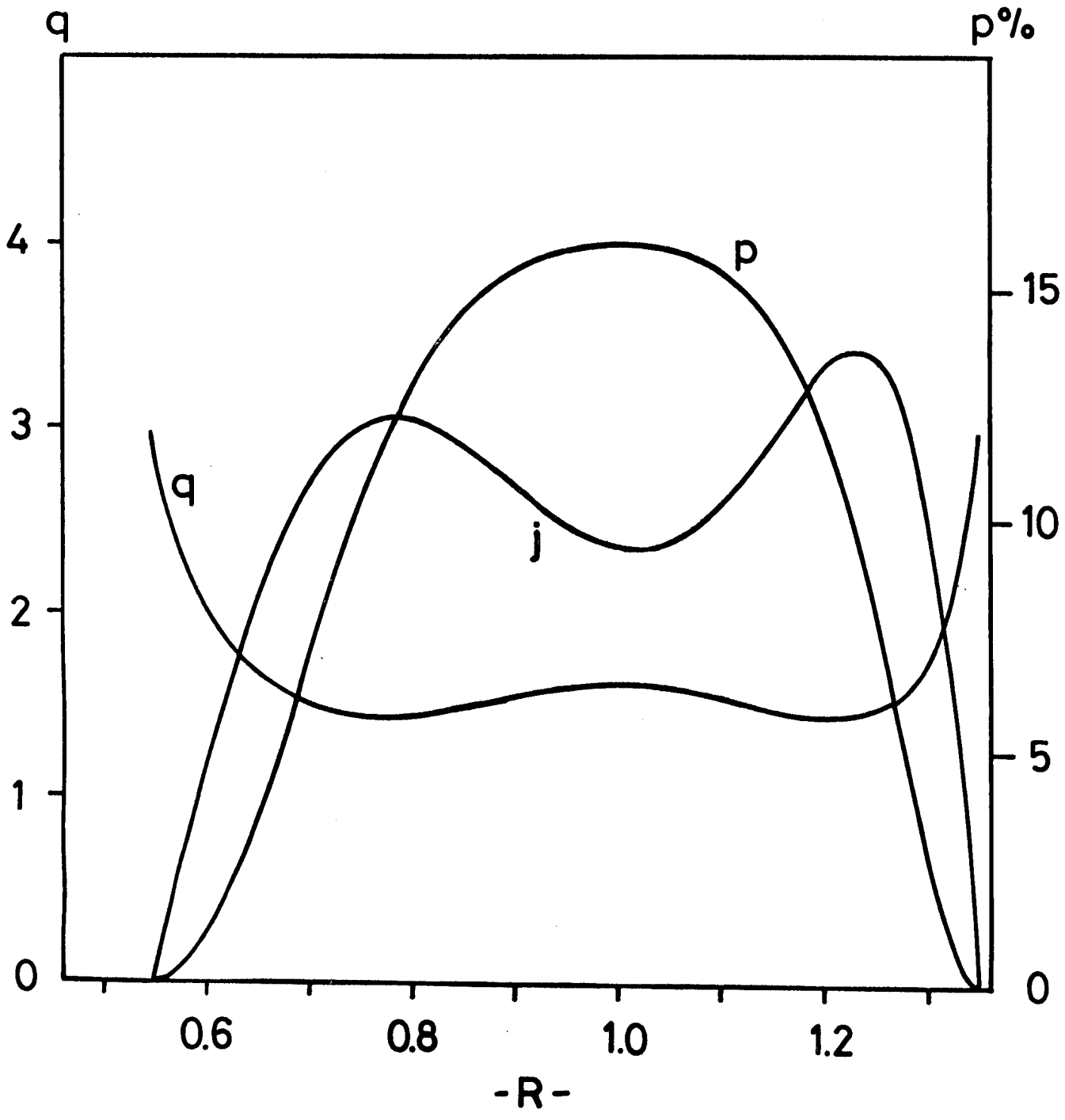

Fig. 9